Finite element schemes
based on energy-stable approximation
for two-fluid flow problems with surface tension

M. Tabata

Abstract. For two-fluid flow problems with surface tension we present finite element schemes based on energy-stable approximation. In the case of no surface tension, those schemes are unconditionally stable in the energy-sense. When there exists surface tension, they are proved to be stable if a quantity remains bounded in the computation. Some numerical results of rising bubble problems show the robustness and applicability of these schemes.

Key words: finite element method, two-fluid flow problems, energy-stability, Navier-Stokes equations, surface tension.

1. Introduction

Multifluid and multiphase flows occur in many scientific and engineering problems. Two key issues in analyzing those flows are to find the position of interfaces separating fluids and to handle the surface tension on the interfaces. Many numerical schemes have been developed and applied to those flow problems, see e.g., [3, 10, 11] and references therein. It is, however, not an easy task to construct numerical schemes, stable and convergent. To the best of our knowledge, there are no numerical schemes whose solutions are proved to converge to the exact one. There are very little discussion even for the stability of schemes. When there is no surface tension, we have developed energy stable finite element schemes from the approach of the density-dependent Navier-Stokes equations and applied them to the Rayleigh-Taylor problem [7, 8]. These schemes are proved to be unconditionally stable in the energy sense. In this formulation the density is treated as a field function solved in the whole domain, and it also works as a level set function.

Here we extend the energy-stable finite element schemes to two-fluid flow problems with surface tension. We consider two-dimensional problems.

The interface curve is represented by a vector-valued function in one parameter, which is approximated by a piecewise linear function, that is, the interface curve is approximated by a polygon. The function is updated by solving numerically ordinary differential equations, an interface-tracking method. The Navier-Stokes equations written in the weak formulation including the surface tension, expressed also in a weak form, are solved in the fixed finite element mesh. We employ the P2/P1 finite element to get the velocity and the pressure, whose convergence theory has been well established [1, 2]. When there exists surface tension, they are proved to be stable if a quantity corresponding to L^2-norm of the curvature is bounded in the computation. In this paper we mainly consider the non-slip boundary conditions. Some preliminary numerical results subject to the slip boundary conditions have been reported in [6].

The contents of this paper are as follows. In Section 2 we formulate two-fluid flow problems with surface tension. In Section 3 finite element schemes for the problems are described. We discuss the stability in the energy sense in Section 4. In Section 5 we show numerical results for bubble rising problems.

Throughout the paper c represents a positive constant independent of the discretization parameters, which may take a different value at each appearance.

2. Two-fluid flow problems with surface tension

Let Ω be a bounded domain in $\mathbf{R}^2$ with piecewise smooth boundary Γ, and T be a positive number. At the initial time $t = 0$ the domain Ω is occupied by two immiscible incompressible viscous fluids; each domain is denoted by Ω_k^0, $k = 1, 2$, whose interface $\partial \Omega_1^0 \cap \partial \Omega_2^0$ is denoted by Γ_{12}^0. We assume that Γ_{12}^0 is a closed curve, which means that one fluid, say, fluid 1, is in the interior of the other fluid 2. At $t \in (0, T)$ the two fluids occupy domains $\Omega_k(t)$, $k = 1, 2$, and the interface curve is denoted by $\Gamma_{12}(t)$. Let ρ_k and μ_k, $k = 1, 2$, be the densities and the viscosities of the two fluids. Let

$$u \colon \Omega \times (0, T) \to \mathbf{R}^2, \quad p \colon \Omega \times (0, T) \to \mathbf{R}$$

be the velocity and the pressure to be found. The Navier-Stokes equations are satisfied in each domain $\Omega_k(t)$, $k = 1, 2$, $t \in (0, T)$,

$$\rho_k\Big\{\frac{\partial u}{\partial t} + (u \cdot \nabla)u\Big\} - \nabla\big[2\mu_k D(u)\big] + \nabla p = \rho_k f, \tag{1}$$

$$\nabla \cdot u = 0, \tag{2}$$

where $f\colon \Omega \times (0,\, T) \to \mathbf{R}^2$ is a given function and $D(u)$ is the strain-rate tensor defined by

$$D_{ij}(u) = \frac{1}{2}\Big(\frac{\partial u_i}{\partial x_j} + \frac{\partial u_j}{\partial x_i}\Big).$$

The interface Γ_{12} is assumed to move with the velocity u at that position, that is, any fluid particle on Γ_{12}^0 remains on the interface $\Gamma_{12}(t)$ at any time t. On $\Gamma_{12}(t)$, $t \in (0,\, T)$, interface conditions

$$[u] = 0, \quad [-pn + 2\mu D(u)n] = \sigma_0 \kappa n \tag{3}$$

are imposed, where $[\,\cdot\,]$ means the difference of the values approached from both sides to the interface, κ is the curvature of the interface, σ_0 is the coefficient of surface tension, and n is the unit normal vector. On the boundary Γ, $t \in (0,\, T)$, the non-slip conditions

$$u = 0 \tag{4}$$

are imposed. Initial conditions at $t = 0$ for the velocity

$$u = u^0 \tag{5}$$

are given.

Our purpose is to construct numerical schemes for this problem. In order to derive a scheme we reformulate the problem as follows: find functions

$$\chi\colon [0,\, 1] \times (0,\, T) \to \mathbf{R}^2, \quad (u,\, p)\colon \Omega \times (0,\, T) \to \mathbf{R}^2 \times \mathbf{R}$$

satisfying for any $t \in (0,\, T)$,

$$\frac{\partial \chi}{\partial t} = u(\chi,\, t), \quad (s \in [0,\, 1]) \tag{6}$$

and (1) and (2) in $\Omega_k(t)$, $k = 1,\, 2$, with interface conditions (3), boundary conditions (4), and initial conditions (5) and

$$\chi(\,\cdot\,,\, 0) = \chi^0, \tag{7}$$

where $\chi^0\colon [0,\, 1] \to \mathbf{R}^2$ is an initial closed curve in Ω. For any t, $\chi(1,\, t) =$

$\chi(0, t)$ and

$$\mathcal{C}(t) = \{\chi(s, t); s \in [0, 1]\}$$

is a closed curve in Ω. $\mathcal{C}(t)$ is nothing but the interface curve at t, and $\Omega_k(t)$, $k = 1, 2$, are defined as the interior and the exterior of $\mathcal{C}(t)$, respectively.

Remark 2.1   (4) can be replaced by the slip boundary conditions,

$$u \cdot n = 0, \quad D(u)n \times n = 0. \tag{8}$$

The following discussion is still valid in this case with a little modification. See Remark 4.5.

3.   Energy-stable finite element approximation

We now present two finite element schemes based on the energy-stable approximation [8] for the problem described in the previous section. We prepare function spaces,

$$X = \{\chi \in H^1(0, 1)^2; \chi(1) = \chi(0)\}, \quad V = H_0^1(\Omega)^2, \quad Q = L_0^2(\Omega).$$

We find a set of functions

$$(\chi, u, p) \colon (0, T) \to X \times V \times Q.$$

Let X_h, V_h, and Q_h be finite-dimensional approximation spaces of X, V, and Q. Let Δt be a time increment and $N_T = \lfloor T/\Delta t \rfloor$. We seek approximate solutions χ_h^n, u_h^n, and p_h^n at $t = n\Delta t$ in X_h, V_h, and Q_h, respectively. More precisely, these approximate function spaces are constructed as follows. Dividing the domain Ω into a union of triangles, we use P2 and P1 finite element spaces for V_h and Q_h, respectively. They are fixed for all time steps n. On the other hand, X_h is composed of functions obtained by the parameterization of polygons. We denote by $\{s_i^n \in [0, 1]; i = 0, \ldots, N_x^n\}$ the set of parameter values such that $s_0^n = 0$ and $s_{N_x^n}^n = 1$ and that $\{\chi_h^n(s_i^n); i = 0, \ldots, N_x^n - 1\}$ are vertices of a polygon. The number N_x^n may change depending on n. We also introduce an auxiliary function space Φ_h consisting of piecewise constant functions on elements. We denote by $\bar{D}_{\Delta t}$ the backward difference operator, i.e.,

$$\bar{D}_{\Delta t} u_h^n = \frac{u_h^n - u_h^{n-1}}{\Delta t}.$$

Scheme I   Find $\{(\chi_h^n,\, u_h^n,\, p_h^n) \in X_h \times V_h \times Q_h; n = 1,\, \ldots,\, N_T\}$ satisfying

$$\bar{D}_{\Delta t}\chi_h^n = \frac{3}{2}u_h^{n-1}(\chi_h^{n-1}) - \frac{1}{2}u_h^{n-2}(\chi_h^{n-1} - \Delta t u_h^{n-1}(\chi_h^{n-1})), \quad \forall s_i^{n-1} \tag{9}$$

$$\left(\rho_h^{n-1}\bar{D}_{\Delta t}u_h^n + \frac{1}{2}u_h^n\bar{D}_{\Delta t}\rho_h^n,\, v_h\right) + a_1(\rho_h^n,\, u_h^{n-1},\, u_h^n,\, v_h)$$
$$+ a_0(\rho_h^n,\, u_h^n,\, v_h) + b(v_h,\, p_h^n)$$
$$= (\rho_h^n \Pi_h f^n,\, v_h) - d_h(\chi_h^n,\, v_h; \mathcal{C}_h^n), \quad \forall v_h \in V_h \tag{10}$$
$$b(u_h^n,\, q_h) = 0, \quad \forall q_h \in Q_h \tag{11}$$

subject to the initial conditions

$$\chi_h^0 = \Pi_h \chi^0, \quad u_h^0 = \Pi_h u^0. \tag{12}$$

Here Π_h is the interpolation operator to the corresponding finite-dimensional space, $(\,\cdot\,,\,\cdot\,)$ shows the inner product in $L^2(\Omega)^2$, and

$$a_1(\rho,\, w,\, u,\, v) = \int_\Omega \frac{1}{2}\rho\big\{[(\nabla\cdot w)u]\cdot v - [(\nabla\cdot w)v]\cdot u\big\}dx,$$

$$a_0(\rho,\, u,\, v) = \int_\Omega 2\mu(\rho)D(u) : D(v)dx,$$

$$b(v,\, q) = -\int_\Omega (\nabla\cdot v)q dx,$$

$$d_h(\chi,\, v; \mathcal{C}_h) = \sum_{i=1}^{N_x} \sigma_0 \bar{D}_{\Delta s}\chi_i \cdot \bar{D}_{\Delta s}v_i \frac{(s_i - s_{i-1})^2}{|\chi_i - \chi_{i-1}|},$$

$$\mu(\rho) = \mu_1 \frac{\rho_2 - \rho}{\rho_2 - \rho_1} + \mu_2 \frac{\rho - \rho_1}{\rho_2 - \rho_1}.$$

$\mathcal{C}_h^n$ is a polygon obtained from χ_h^n. (9) is the Adams-Bashforth approximation of (6). The number of particles on the interface at time step n is denoted by N_x^n. We control N_x^n so that the particles may be distributed quasi-uniformly, i.e., we add or delete particles by judging distances of neighboring particles. A more precise description of (9) is as follows. We denote X_h at time step n by $X_h(N_x^n)$. Let $\chi_h^{n-1/2} \in X_h(N_x^{n-1})$ be an intermediate function such that for $i = 0,\, \ldots,\, N_x^{n-1}$ at s_i^{n-1},

$$\frac{\chi_h^{n-1/2} - \chi_h^{n-1}}{\Delta t} = \frac{3}{2}u_h^{n-1}(\chi_h^{n-1}) - \frac{1}{2}u_h^{n-2}(\chi_h^{n-1} - \Delta t u_h^{n-1}(\chi_h^{n-1})). \tag{13}$$

Adding and deleting particles to $\chi_h^{n-1/2}$, we get $\chi_h^n \in X_h(N_x^n)$. Once χ_h^n is known, we can define Ω_{hk}^n, $k = 1, 2$, as the interior and the exterior of the polygon $\mathcal{C}_h^n$, respectively. In (10) $\rho_h^n \in \Phi_h$ is an auxiliary function defined by

$$\rho_h^n(K) = \rho_k$$

for the element K included in Ω_{hk}^n. For the element K intersecting with $\mathcal{C}_h^n$, $\rho_h^n(K)$ is defined as the density averaged by the areas occupied by ρ_k. Equations (10) and (11) are approximations of the corresponding weak forms, which are derived as follows. Let $\rho\colon \Omega \times (0, T) \to \mathbf{R}$ be a function governed by the convection equation,

$$\frac{\partial \rho}{\partial t} + u \cdot \nabla \rho = 0. \tag{14}$$

Although the density of our problem is discontinuous, we suppose that it is approximated by a function having the first order derivatives. We multiply (14) by $u/2$, and add it to (1). Multiplying the equation by a test function $v \in V$, integrating by parts, and incorporating the interface conditions (3) and the boundary conditions (4), we obtain

$$\left(\rho \frac{\partial u}{\partial t} + \frac{1}{2} u \frac{\partial \rho}{\partial t}, \, v \right) + a_1(\rho, \, u, \, u, \, v) + a_0(\rho, \, u, \, v) + b(v, \, p)$$
$$= (\rho f, \, v) - d(\chi, \, v; \mathcal{C}), \tag{15}$$

where

$$d(\chi, \, v; \mathcal{C}) \equiv \int_{\mathcal{C}} \sigma_0 \frac{\partial \chi}{\partial \ell} \cdot \frac{\partial v}{\partial \ell} d\ell$$

is a bilinear form derived from the surface tension, and ℓ is the arclength of the interface curve $\mathcal{C}$. Here we have used the fact that κn is equal to the second derivative of χ with respect to ℓ and the integration by parts on the closed curve $\mathcal{C}$. The weak formulation of (2) is nothing but

$$b(u, \, q) = 0,$$

where $q \in Q$ is a test function. (10) and (11) consist of an energy-stable finite element scheme developed in [8] when there is no term d_h. The bilinear form d_h is an approximation of d.

Scheme II   We add the term

$$\Delta t \ d_h(u_h^n, \ v_h; \mathcal{C}_h^n)$$

to the left-hand side of (10). The other parts are same as Scheme I.

Since the fluids are incompressible, each area $\Omega_k(t)$ remains constant. In order to keep this property we correct $\chi_h^{n-1/2}$ after (13) by expanding or shrinking $\mathcal{C}_h^{n-1/2}$ from the centroid. Thus our schemes keep the property $\text{meas}\,\Omega_{hk}^n = \text{meas}\,\Omega_{hk}^0$ for all n.

Remark 3.1   (i)   In deriving the weak form (15), we have assumed that ρ had the first order derivatives. In the scheme (10), however, we do not need any regularity on ρ_h, which enables us to use $\rho_h \in \Phi_h$.
(ii)   Scheme II is obtained when the curvature of the interface is computed implicitly from χ_h^{n+1}, which is approximated by

$$\chi_h^n + \Delta t u_h^n.$$

For the idea of the introduction of this term we refer to [9]. Scheme II is more stable than Scheme I, which is recognized by numerical results in Section 5.
(iii)   For the first step $n = 1$ we replace (9) by the Euler method.

4.   Stability in energy

Now we consider the stability in energy of Schemes I and II. We equip the function spaces V_h, and Q_h with the norms $H^1(\Omega)^2$ and $L^2(\Omega)$, respectively. They are denoted simply by $|| \cdot ||_1$ and $|| \cdot ||_0$. In (10) the functions ρ_h^{n-1}, ρ_h^n, u_h^{n-1}, and χ_h^n are all known. The system of (10) and (11) is a generalized Stokes problem in u_h^n and p_h^n. Since the P2/P1 element satisfies the inf-sup condition, the problem is uniquely solvable.

For a series of functions $\phi_h = \{\phi_h^n\}_{n=0}^{N_T}$ in a Banach space W we prepare norms defined by

$$||\phi_h||_{\ell^\infty(W)} \equiv \max\{||\phi_h^n||_W; \ 0 \le n \le N_T\},$$

$$||\phi_h||_{\ell^2(W)} \equiv \Big\{\Delta t \sum_{n=0}^{N_T} ||\phi_h^n||_W^2\Big\}^{1/2}.$$

For a closed curve $\mathcal{C}$ we denote the L^2-norm of a function v on the curve by

$$||v||_{0,\mathcal{C}} = \sqrt{\int_{\mathcal{C}} |v|^2 d\ell}.$$

Since $\mathcal{C}_h^n$ is a polygon, we can apply the trace theorem; there exists a positive constant c such that for any $v \in H^1(\Omega)$ it holds that

$$||v||_{0,\mathcal{C}_h^n} \leq c||v||_1.$$

In general, the constant c depends on the length and the smoothness of the curve. We assume that it does not depend on h and n and that the curve is not self-intersecting for simplicity.

Hypothesis 4.1   (i) $\mathcal{C}_h^n$ is not self-intersecting.
(ii)   There exists a positive constant c_0 independent of h and n such that

$$||v||_{0,\mathcal{C}_h^n} \leq c_0||v||_1 \quad (\forall v \in H^1(\Omega)). \tag{16}$$

Remark 4.2   (i)   If u is continuous and satisfies the Lipschitz condition with respect to x, the ordinary differential equation (6) has a unique solution $\chi(s)$ for each s, which implies that $\mathcal{C}(t)$ is not self-intersecting. On the other hand, the approximation $\mathcal{C}_h^n$, constructed from the solution χ_h^n of (9), may be self-intersecting, especially when Δt is large.
(ii)   If $\mathcal{C}_h^n$ is divided into a number (independent of h and n) of parts and if the gradients $\nabla \chi_h^n$ are uniformly (in h and n) bounded on each part, then assumption (16) is satisfied. Although (16) looks like a rather mild assumption, it seems not so easy to give a sufficient condition for it on our schemes I and II.

Let $\chi_h \in X_h$ and $\{s_i \in [0, 1]; i = 0, \ldots, N_x\}$ be the set of parameters, $s_0 = 0$, $s_{N_x} = 1$, $\chi_h(1) = \chi_h(0)$. We define the quantity $||\chi_h||_{H^2_{0,h}(\mathcal{C}_h)}$ by

$$||\chi_h||_{H^2_{0,h}(\mathcal{C}_h)} = \Big\{ \sum_{i=0}^{N_x-1} |(D^2_{\Delta\ell}\chi_h)(s_i)|^2 \ell_i \Big\}^{1/2}, \tag{17}$$

where

$$\ell_i = \frac{1}{2}(\ell_{i+1/2} + \ell_{i-1/2}), \quad \ell_{i+1/2} = |\chi_h(s_{i+1}) - \chi_h(s_i)|,$$

$$(D^2_{\Delta\ell}\chi_h)(s_i) = \Big(\frac{\chi_h(s_{i+1}) - \chi_h(s_i)}{\ell_{i+1/2}} - \frac{\chi_h(s_i) - \chi_h(s_{i-1})}{\ell_{i-1/2}} \Big) \Big/ \ell_i.$$

Proposition 4.2 *Suppose that* Schemes I *or* II *has a solution* (ρ_h^n, u_h^n, p_h^n) $\in \Phi_h \times V_h \times Q_h$, $n = 0, \ldots, N_T$, *and that* Hypothesis 4.1 *is satisfied. Then there exists a positive constant c independent of h and Δt such that*

$$||\sqrt{\rho_h}u_h||_{\ell^\infty(L^2)}, ||\sqrt{\mu_h}D(u_h)||_{\ell^2(L^2)}$$

$$\leq c\Big\{||\sqrt{\rho_h^0}u_h^0||_0 + ||\sqrt{\rho_h}\,\Pi_h f||_{\ell^2(L^2)} + \frac{c_0\sigma_0}{\sqrt{\mu_{\min}}}||\chi_h||_{\ell^2(H^2_{0,h}(\mathcal{C}_h))}\Big\}, \quad (18)$$

where $\mu_{\min} = \min(\mu_1, \mu_2)$.

Proof. We substitute $v_h = u_h^n$ in (10). The first term is equal to

$$\Big(\rho_h^{n-1}\bar{D}_{\Delta t}u_h^n + \frac{1}{2}u_h^n\bar{D}_{\Delta t}\rho_h^n, \, u_h^n\Big)$$

$$= \bar{D}_{\Delta t}\Big(\frac{1}{2}||\sqrt{\rho_h^n}u_h^n||_0^2\Big) + \frac{1}{2}||\sqrt{\Delta t}\sqrt{\rho_h^{n-1}}\bar{D}_{\Delta t}u_h^n||_0^2.$$

The second term vanishes. The third term is estimated as

$$a_0(\rho_h^n, \, u_h^n, \, u_h^n) \geq \frac{1}{2}a_0(\rho_h^n, \, u_h^n, \, u_h^n) + \mu_{\min}||D(u_h^n)||_0^2$$

$$\geq \frac{1}{2}a_0(\rho_h^n, \, u_h^n, \, u_h^n) + c_1^2\mu_{\min}||u_h^n||_1^2,$$

where c_1 is a positive constant in the Korn inequality. The fourth term vanishes from (11). The first term of the right-hand side is evaluated as

$$|(\rho_h^n\Pi_h f^n, \, u_h^n)| \leq \epsilon||\sqrt{\rho_h^n}u_h^n||_0^2 + \frac{1}{4\epsilon}||\sqrt{\rho_h^n}\Pi_h f^n||_0^2$$

where ϵ is any positive constant. The second term of the right-hand side is rewritten as

$$-d_h(\chi_h^n, \, u_h^n; \mathcal{C}_h^n) = \sum_{i=0}^{N_x^n-1} \sigma_0(D_{\Delta\ell}^2\chi_h^n)(s_i^n)u_h^n(s_i^n)\ell_i$$

by means of summation by parts. The right-hand side is evaluated by

$$\sigma_0||\chi_h^n||_{H^2_{0,h}(\mathcal{C}_h)}\Big\{\sum_{i=0}^{N_x^n-1} u_h^n(s_i^n)^2\ell_i\Big\}^{1/2}$$

$$\leq c\sigma_0||\chi_h^n||_{H^2_{0,h}(\mathcal{C}_h)}||u_h^n||_{0,\mathcal{C}_h^n}$$

$$\leq cc_0\sigma_0||\chi_h^n||_{H^2_{0,h}(\mathcal{C}_h)}||u_h^n||_1$$

$$\le cc_0^2 \sigma_0^2 \frac{1}{c_1^2 \mu_{\min}} ||\chi_h^n||_{H_{0,h}^2(\mathcal{C}_h)}^2 + c_1^2 \mu_{\min} ||u_h^n||_1^2.$$

Combining these estimates and applying the discrete Gronwall inequality, we get (18). In Scheme II we have another term $\Delta t d_h(u_n^n, u_h^n; \mathcal{C}_H^n)$ in the left-hand side, which increases the stability. $\qquad \square$

Remark 4.4 (i) There are correspondences,

$$||\sqrt{\rho_h} u_h||_{\ell^\infty(L^2)} \sim \max\left\{ \left\{ \int_\Omega \rho(t)|u(t)|^2 dx \right\}^{1/2}; 0 \le t \le T \right\},$$

$$||\chi_h||_{\ell^2(H_{0,2}^2(\mathcal{C}_h))} \sim \left\{ \int_0^T dt \int_{\mathcal{C}(t)} \kappa^2 d\ell \right\}^{1/2}.$$

Hence, (18) is a discrete version of the fact that the total energy remains bounded if the curvature is bounded in L^2-norm.
(ii) The result (18) is still valid in the case where $\sigma_0 = 0$. If there is no surface tension, the total energy remains bounded.

Remark 4.5 Proposition 4.2 is valid also in the case of the slip boundary conditions (8). Then we impose the condition $(v_h \cdot n)(P) = 0$ at nodes on Γ for the function v_h in V_h. When Ω is a circle, the Korn inequality does not hold. In this case we have to impose another condition to V_h such that V_h is orthogonal to the rigid movement. For the details we refer to [4].

5. Numerical results

We show numerical results of rising bubble problems. Let $\Omega \equiv (0, 1) \times (0, 2)$ and $T = 10$. We set

$$\chi^0(s) = \left(\frac{1}{2} + \frac{1}{5} \cos 2\pi s, \frac{2}{5} + \frac{1}{5} \sin 2\pi s \right).$$

The initial domains Ω_1^0 and Ω_2^0 are shown in Fig. 1. We take the following values,

$$(\rho_1, \mu_1) = (0.1, 1), \quad (\rho_2, \mu_2) = (100, 2)$$

and the initial velocity and the gravity,

$$u^0 = (0, 0)^T, \quad f = (0, -1)^T.$$

Non-slip boundary conditions (4) are imposed. We use three meshes, $\mathcal{T}_{1/16}$, $\mathcal{T}_{1/32}$, and $\mathcal{T}_{1/64}$. In $\mathcal{T}_{1/n}$ the sides AB and CD are divided into n equal seg-
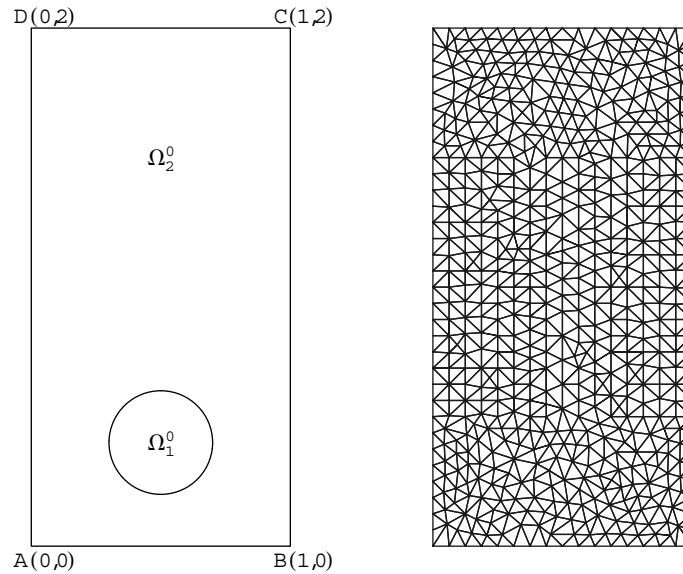
Fig. 1.   Statement of the problem and a mesh $\mathcal{T}_{1/16}$.

ments, and the other sides are divided into $2n$. The total element numbers are 1,138, 4,580, and 18,444, respectively. In Fig. 1 mesh $\mathcal{T}_{1/16}$ is shown. We use a simple notation $K(\mathcal{C}_h)$ defined by

$$K(\mathcal{C}_h) = ||\chi_h||_{\ell^2(H^2_{0,h}(\mathcal{C}_h))}.$$

5.1.   The comparison of Schemes I and II

We compare the stability property of Schemes I and II. When $\sigma_0 = 0$, both schemes are identical and unconditionally energy-stable by Proposition 4.2, i.e., for any $\Delta t > 0$

$$\max \left\{ \int_{\Omega} \rho_h^n |u_h^n|^2 dx; n = 0, \ldots, N_T \right\} \le M_0,$$

where M_0 is a positive constant. In the case of $\sigma_0 > 0$ we see Scheme II is more stable than Scheme I. Letting $\sigma_0 = 1.0$, we solve the problem on mesh $\mathcal{T}_{1/32}$. We set $\Delta t = 1/8$. In Scheme I the computed interface becomes serrate and the value $||\chi_h^n||_{H^2_{0,h}(\mathcal{C}_h)}$ grows up. We cannot simulate the phenomenon. In Scheme II we can obtain the solution depicted in Fig. 2, where interface
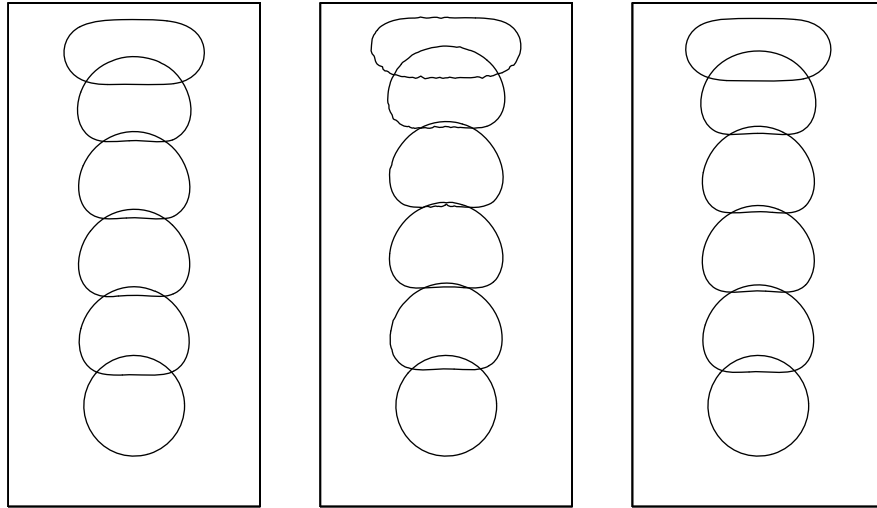
Fig. 2.   Interfaces at $t = 0, 2, \ldots, 10$ for $\Delta t = 1/8$ by Scheme II (left), and for
$\Delta t = 1/16$ by Scheme I (center) and by Scheme II (right). $\sigma_0 = 1$.

curves are shown at $t = 0, 2, 4, 6, 8, 10$. $K(\mathcal{C}_h)$ is equal to 49.7. When $\Delta t = 1/16$ we can get the solutions for both schemes. While small jags are found in the interface curves obtained by Scheme I at $t = 6, 8, 10$, the curves obtained by Scheme II are smooth. $K(\mathcal{C}_h)$ is equal to 88.16 and 45.52 for Schemes I and II, respectively. Since Scheme II is more stable than Scheme I, we use Scheme II hereafter.

5.2.   The dependence on the subdivision

Setting $\sigma_0 = 1$, we compare numerical results obtained from meshes $\mathcal{T}_{1/16}$, $\mathcal{T}_{1/32}$, and $\mathcal{T}_{1/64}$. Time increment Δt is chosen to be $1/16$, $1/32$, and $1/64$, respectively. The results are shown in Fig. 3. From these figures Hypothesis 4.1 seems to be satisfied. $K(\mathcal{C}_h)$ is equal to 34.09, 45.88 and 55.66, respectively.

5.3.   The effect of the coefficient of surface tension

We use mesh $\mathcal{T}_{1/32}$ and set $\Delta t = 1/32$. We take $\sigma_0 = 0.0, 0.1, 1.0, 2.0$. Their interface curves are shown in Figs. 4 and Fig. 3 ($\sigma_0 = 1$). As σ_0 becomes larger, the shape of the interface becomes more round because of larger surface tension. Fig. 5 shows the elevations of the pressure at $t = 5.0$.
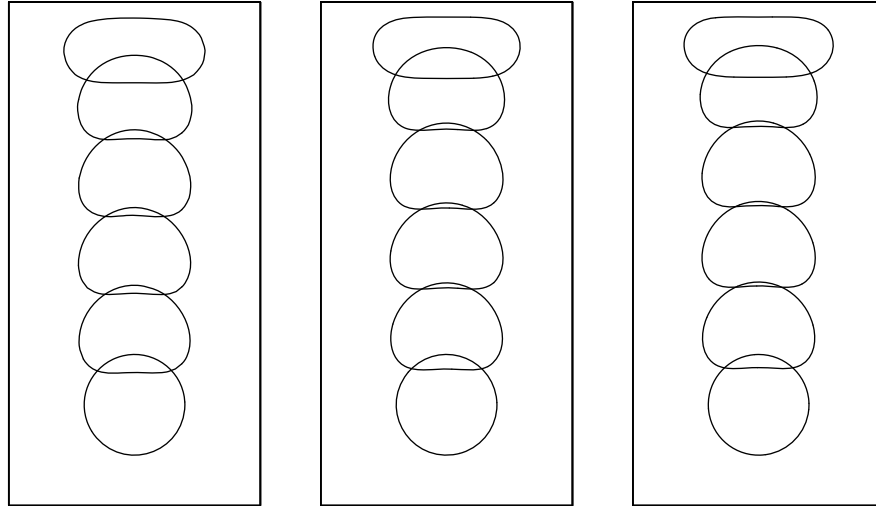
Fig. 3. Interfaces at $t = 0, 2, \ldots, 10$ solved on $\mathcal{T}_{1/16}$ (left), $\mathcal{T}_{1/32}$ (center), and $\mathcal{T}_{1/64}$ (right). $\sigma_0 = 1$.
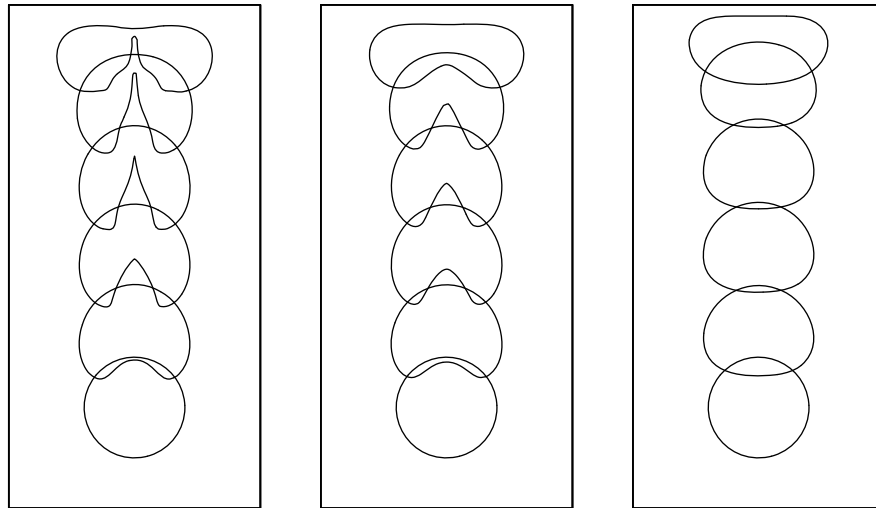

Fig. 4. Interfaces at $t = 0, 2, \ldots, 10$. $\sigma_0 = 0$ (left), $\sigma_0 = 0.1$ (center), and $\sigma_0 = 2$ (right).
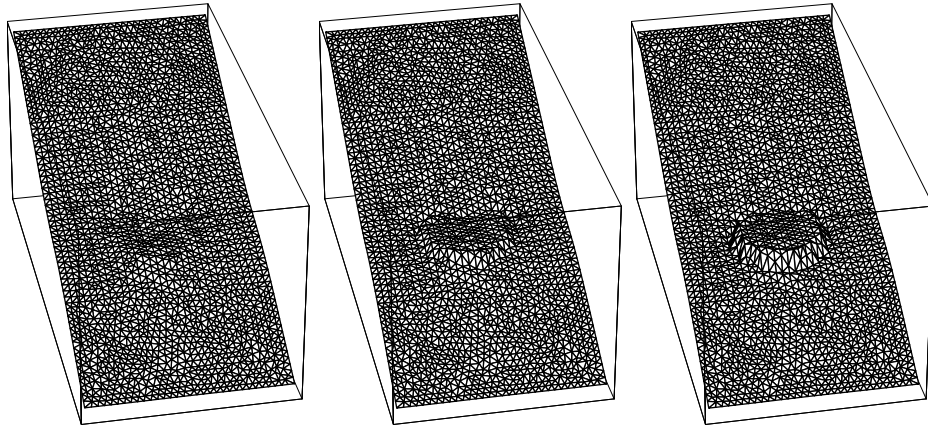
Fig. 5.   Elevations of the pressure at $t = 5.0$. $\sigma_0 = 0.0$ (left), 1.0 (center), 2.0 (right).
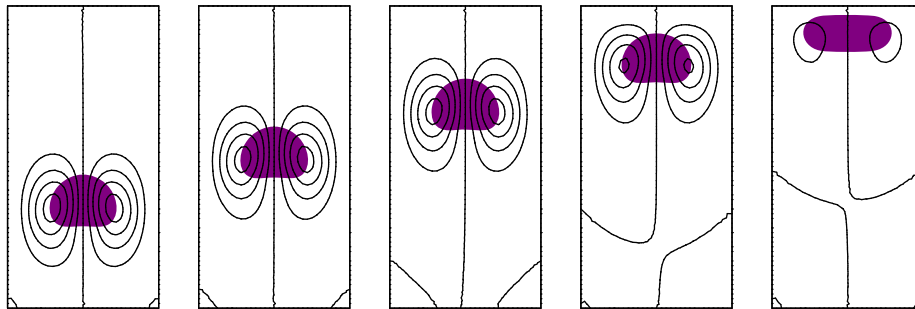

Fig. 6.   Interfaces and streamlines at $t = 2, 4, \ldots, 10$ subject to the non-slip boundary conditions.

In these figures the front side is CD. When σ_0 becomes large, the pressure in Ω_1 increases. In these four cases $K(\mathcal{C}_h)$ is equal to 80.21, 58.57, 45.88 and 43.00, respectively.

5.4.   The effect of boundary conditions

We consider problems of non-slip and slip boundary conditions. We use mesh $\mathcal{T}_{1/32}$ and set $\Delta t = 1/32$, and $\sigma_0 = 1.0$. Figs. 6 and Fig. 7 show the interfaces and the streamlines. The intervals of streamlines are same for both figures. In the case of the slip boundary conditions the flow pattern is larger and the bubble goes up faster, which induces the lower pressure in
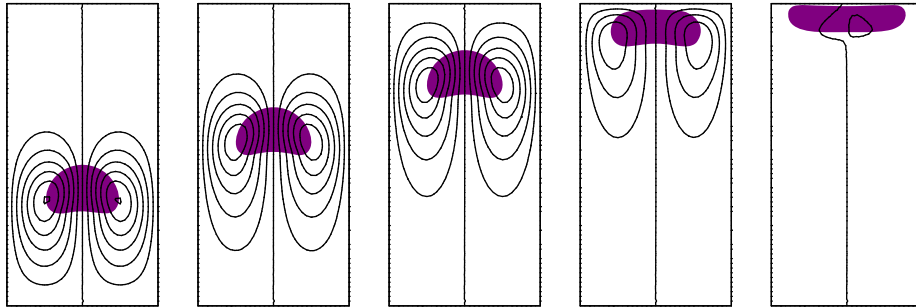
Fig. 7.   Interfaces and streamlines at $t = 2, 4, \ldots, 10$ subject to the slip boundary
          conditions.

the rear and the hollow in the lower part of the interface. The value $K(\mathcal{C}_h)$
is equal to 46.44 in the slip boundary condition case. $K(\mathcal{C}_h)$ in the non-slip
boundary condition case is 45.88 as mentioned in the previous subsection.

6.   Concluding remarks

We have developed finite element schemes for two-fluid flow problems
with surface tension based on energy-stable approximation and analysed
the stability. In the case of no surface tension, the schemes are stable
in the energy sense. When surface tension is present, we have shown a
numerical criterion for the schemes to be stable in the energy sense. We
have examined the criterion in bubble rising problems. These are robust
and mathematically sound schemes.

References

[1]   Brezzi F. and Fortin M., *Mixed and Hybrid Finite Element Methods.* Springer, New
        York, 1991.
[2]   Girault V. and Raviart P.A., *Finite Element Methods for Navier-Stokes Equations,
        Theory and Algorithms.* Springer, New York, 1986.

[3]   Osher S. and Fedkiw R.P., *Level set methods: an overview and some recent results.*
        Journal of Computational Physics vol. 169, 2001, pp. 463–502.

[4]   Tabata M., *Uniform solvability of finite element solutions in approximate domains.*
        Japan Journal of Industrial and Applied Mathematics **18** (2001), 567–585.

[5]   Tabata M., *Numerical simulation of Rayleigh-Taylor problems by an energy-stable
        finite element scheme.* in "Proceedings of The Fourth International Workshop on
        Scientific Computing and Applications", (Guo B.-Y. and Shi Z.-C., eds), Science
        Press, Beijing, 2007, pp. 63–73.

[6]   Tabata M., *Energy stable finite element schemes and their applications to two-
        fluid flow problems.* in "Proceedings of European Conference on Computational
        Fluid Dynamics", (Wesseling P., Oñate E. and Périaux J., eds), TU Delft, The
        Netherlands, 2006, pp. 379/1–10.

[7]   Tabata M. and Fukushima Y., *A finite element approximation to density-dependent
        Navier-Stokes equations and its application to Rayleigh-Taylor instability prob-
        lem.* in "Advances in Computational & Experimental Engineering and Sciences",
        (Sivakumar S.M. *et al.*, eds), Tech Science Press, Forsyth, 2005, pp. 455–460.

[8]   Tabata M. and Kaizu.S, *Finite element schemes for two-fluids flow problems.* in
        "Proceedings of The Seventh China-Japan Seminar on Numerical Mathematics",
        (Shi Z.-C. and Okamoto H., eds), Science Press, Beijing, 2006, pp. 139–148.

[9]   Tabata M. and Tagami D., *A finite element analysis of a linearized problem of the
        Navier-Stokes equations with surface tension.* SIAM Journal on Numerical Analysis
        38 (2000), 40–57.

[10]   Tezduyar T.E., Behr M. and Liou J., *A new strategy for finite element computations
        involving boundaries and interfaces - the deforming-spatial-domain /space-time pro-
        cedure*: I Computer Methods in Applied Mechanics and Engineering **94** (1992),
        339–351.

[11]   Tryggvason G., Bunner B., Esmaeeli A., Juric D., Al-Rawahi N., Tauber W., Han J.,
        Nas S. and Jan Y.-J., *A front-tracking method for the computations of multiphase
        flow.* Journal of Computational Physics **169** (2001), 708–759.

Faculty of Mathematics
Kyushu University
Fukuoka, 812-8581, Japan
E-mail: tabata@math.kyushu-u.ac.jp